Arabian Journal of Chemistry (2019) **12**, 3628–3638

King Saud University

Arabian Journal of Chemistry

www.ksu.edu.sa
www.sciencedirect.com

ORIGINAL ARTICLE

Recovery of molybdenum oxyanions using macroporous copolymer grafted with diethylenetriamine

Bojana M. Ekmeščić [a], Danijela D. Maksin [b], Jelena P. Marković [b], Zorica M. Vuković [c], Radmila V. Hercigonja [d], Aleksandra B. Nastasović [a,*], Antonije E. Onjia [b]

[a] *University of Belgrade, Institute of Chemistry Technology and Metallurgy, Department of Chemistry, Njegoševa 12, Belgrade, Serbia*
[b] *University of Belgrade, Vinča Institute of Nuclear Sciences, P.O. Box 522, 11001 Belgrade, Serbia*
[c] *University of Belgrade, Institute of Chemistry Technology and Metallurgy, Department of Catalysis and Chemical Engineering, Njegoševa 12, Belgrade, Serbia*
[d] *University of Belgrade, Faculty of Physical Chemistry, Studentski trg 12-16, 11001 Belgrade, Serbia*

Received 5 August 2015; accepted 16 November 2015
Available online 12 December 2015

KEYWORDS

Macroporous crosslinked copolymer;
Mo(VI) recovery;
Diethylenetriamine;
Sorption kinetics

Abstract The presented study describes macroporous crosslinked poly(glycidyl methacrylate-*co*-ethylene glycol dimethacrylate) [PGME] functionalized with diethylenetriamine [PGME-deta] as a potential recovery agent for Mo(VI) oxyanions from aqueous solutions. Sorption studies were carried out by varying experimental conditions (pH, time, concentration, temperature). Kinetics of Mo(VI) sorption was investigated in batch (static) experiments, in the temperature range 298–343 K. Sorption dynamics data were fitted to seven chemical-reaction and particle-diffusion models. The kinetics studies showed that Mo(VI) sorption adhered to the pseudo-second-order model under all investigated operating conditions. The sorption kinetics was determined to be governed by both the intraparticle diffusion and the external film diffusion to a lesser extent. The temperature rise promotes the molybdate species removal, with the maximum experimental

* Corresponding author. Tel.: +381 11 2635 839; fax: +381 11 2636 061.
E-mail addresses: anastaso@chem.bg.ac.rs, anastasovic@yahoo.com (A.B. Nastasović).
Peer review under responsibility of King Saud University.

Production and hosting by Elsevier

http://dx.doi.org/10.1016/j.arabjc.2015.11.010

uptake capacity of 4.02 mmol g^{-1} at 298 K, at the selected pH which is consistent with the predominance range of hydrolized polynuclear Mo(VI) forms and optimum electrostatic attraction.

1. Introduction

Molybdenum (Mo) is a relatively rare chemical element that became of great importance as an alloying element in steel production and as an inhibitor for steel corrosion due to its low toxicity (Atia et al., 2008). It is a transition metal that occurs in the range of oxidation states from +2 to +6 with the predominance of Mo(IV) and Mo(VI) species. In aqueous environment, molybdenum exists mainly in the form of molybdate and/or other molybdenum polyanions, depending on the solution pH and the initial concentration of metal (Navarro et al., 2003). At low concentrations, Mo is an important nutrient for normal growth of humans, animals and plants. This element takes part in important biochemical processes; it is an essential element in correlation with a variety of metalloenzymes and consequent metabolic functions (Soetan et al., 2010). Elevated doses of molybdenum can be detrimental for human health and in 2011, WHO (World Health Organization) has recommended a health-based reference value of 70 μg L^{-1} Mo permissible in drinking water (World Health Organization, 2011).

High molybdenum levels can cause serious health problems, such as anemia, liver and kidney abnormalities, bone and joint deformities, and sterility (Namasivayam and Sengeetha, 2006). Thus, efficient separation and remediation technologies are drastically needed.

Different techniques, such as co-precipitation, solvent extraction and reverse osmosis are used for molybdenum removal from surface and groundwater (Atia et al., 2008). Among the approaches that have been elaborated for this purpose, adsorption falls into the category of the most effective and the simplest. A number of different types of sorbents (Al-Dalama et al., 2005; Cruywagen and de Wet, 1988; Pagnanelli et al., 2011; Sabine and Forster, 1998; Xu et al., 2006) were used for molybdenum removal from aqueous solutions. Macroporous crosslinked copolymers of glycidyl methacrylate (GMA) and ethylene glycol dimethacrylate (EGDMA), PGME, in the shape of regular beads and the specific pore size are very interesting due to the reactive character of their epoxy groups (Jovanović et al., 1994). For example, PGME functionalized with diethylene diamine, PGME-deta, was already proven to be an adaptable sorbent for removal of precious and heavy metals (Maksin et al., 2012; Nastasović et al., 2004, 2007). Additionally, it is easily synthesized and handled, non-toxic and inexpensive compared to the most popular universal sorbents such as active carbon or those specially synthesized, maintaining an excellent sorption capacity for the Mo oxyanion species.

Considering the wide-spread use of both radioactive and inactive molybdenum isotopes, present as hazardous pollutants in various effluents, there are not many published papers dealing with the issue of Mo sorption, to the best of our knowledge. The Mo removal from ground and wastewaters is of great importance for the environment remediation and thus protection of the inhabitant life forms.

In this paper, macroporous PGME copolymer synthesized by suspension copolymerization and functionalized with diethylenetriamine, PGME-deta, was the material evaluated as a potential Mo (VI) sorbent. Parameters investigated for their influence on Mo (VI) oxyanion sorption on PGME-deta from aqueous solutions include pH, contact time and temperature. All Mo(VI) concentrations in both solid and liquid media are expressed as total metal (mmol) regardless of the structure of the molybdenum species, while the sorbate is referred to as the molybdate oxyanion as a general term.

Sorption kinetic data were analyzed using seven kinetic models [pseudo-first-order (PFO), pseudo-second-order (PSO), Elovich, intraparticle diffusion (IPD), Bangham, Boyd and Mckay] to determine the nature of sorption kinetics and the rate limiting step for molybdate oxyanion sorption by amino-functionalized PGME.

2. Experimental

2.1. Materials and methods

All the chemicals used for copolymer synthesis were analytical grade products and used as received: glycidyl methacrylate (Merck), ethylene glycol dimethacrylate (Fluka), diethylenetriamine (Merck), 2,2′-azobisiso-butyronitrile, AIBN (Merck), poly(N-vinyl pyrrolidone) (Kollidon 90, BASF), cyclohexanol (Merck) and 1-tetradecanol (Merck). Molybdate (VI) solutions were prepared from reagent grade ammonium molybdate tetrahydrate, $(NH_4)Mo_7O_{24}{\cdot}4H_2O$ (Sigma–Aldrich), using deionized water (Milli-Q Millipore, 18 MΩ cm^{-1} conductivity).

The carbon, hydrogen and nitrogen contents of amino-functionalized macroporous sample were analyzed for using the Vario EL III device (GmbH Hanau Instruments, German).

Infrared spectra were taken in attenuated total reflection (ATR) mode using a Nicolet 380 FTIR spectrometer equipped with a Smart Orbit™ ATR attachment containing a single-reflection diamond crystal. The angle of incidence was 45°. Typically, 32 scans were performed for each spectrum at a resolution of 4 cm^{-1}.

The energy dispersive spectroscopic (EDS) analysis was performed on Jeol JSM 5800 instrument operating at 20 kV.

The pH values of the working solutions were adjusted by Hanna HI 2210 (a microprocessor-based pH and temperature bench meter).

The concentrations of Mo(VI) were determined by inductively coupled plasma optical emission spectrometry ICP-OES (Perkin Elmer, Model ICP 400). Standard statistical methods were applied to calculate the mean values and standard deviations for each set of data. All experiments were repeated in triplicate or more if necessary. Relative standard deviations were less than or equal to 5%.

2.2. PGME preparation and functionalization with diethylenetriamine

Macroporous crosslinked GMA and EGDMA copolymer was obtained through suspension copolymerization (60 mass % of GMA and 40 mass% of EGDMA in monomer phase) in the presence of inert component as described previously (Hercigonja et al., 2012). Particles with diameters in the range 0.15–0.30 mm were functionalized with diethylenetriamine using the procedure described elsewhere (Hercigonja et al., 2012). The functionalized sample was filtered, washed with ethanol, dried and labeled as PGME-deta

(additional label -deta designates sample functionalized with diethylenetriamine).

2.3. Sorption experiments

The effects of pH, contact time, initial concentration of Mo (VI) ions and temperature on the sorption capacity of PGME-deta were investigated in aqueous solutions in batch experimental mode and static conditions. The same volume of the solution (V = 50.0 cm^3) and copolymer mass of 50 mg was used in all the experiments.

The effect of pH was studied at room temperature (298 K). The desired pH was adjusted by adding the appropriate amounts of 1 M HCl; pH values were monitored with the pH-meter. The experiments lasted 300 min while the initial Mo(VI) concentration (C_i) was 0.1 M.

The influence of initial metal concentration (C_i = 0.01–0.1 M) on sorption was evaluated at room temperature (298 K). For the contact time studies, the aliquots were withdrawn at the predetermined time intervals (0–1440 min) at the initially adjusted pH value of 2.0. The influence of temperature on molybdenum sorption on PGME-deta was investigated with the selected initial Mo(VI) concentration (C_i = 0.1 M) at four different temperatures (298, 313, 328 and 343 K) and at pH = 2.0. These experiments were carried out with the same mass of PGME-deta (m = 50 mg) up to 360 min. Sample aliquots were regularly withdrawn and analyzed for metal content. All Mo(VI) solution content measurements were performed with ICP-OES.

The sorbed amount of Mo(VI) at any time t, per unit mass of the sorbent beads (m, g) was calculated by the following mass balance relationship:

$$Q_t = \frac{(C_i - C_t)V}{m} \quad (1)$$

where Q_t is sorption capacity (mmol g^{-1}), C_i and C_t are concentrations of Mo(VI) ions in the initial solution and in aqueous solution at time t (min), and V is the volume of the aqueous phase (dm^3).

3. Results and discussion

3.1. Characterization of sorbents

The suspension copolymerization in the presence of inert component (mixture of cyclohexanol and 1-tetradecanol) was the means of acquiring macroporous crosslinked PGME, which was subsequently amino-functionalized with diethylenetriamine (PGME-deta).

Relevant porosity parameters of the sample PGME-deta were as follows: specific surface area, $S_{s,Hg}$ = 55 m^2 g^{-1}; pore diameter which corresponds to half of pore volume, $D_{V/2}$ = 107 nm and specific pore volume, V_S = 0.91 cm^3 g^{-1} (Hercigonja et al., 2012). On the basis of the elemental analysis of PGME-deta (C, 52.4%; H, 8.1% and N, 9.1%), amino group concentration was calculated to be 5.01 mmol g^{-1}.

3.2. Effect of pH

The initial pH of aqueous solution is a critical process parameter in metal sorption of metal, since the pH value determines the speciation of in this case Mo(VI) oxyanions as well as the surface charge of the sorbent in the aqueous solution. Depending on the pH and the total metal concentration, Mo(VI) could exist as anionic mononuclear and polynuclear species (Atia et al., 2008). In alkaline and neutral aqueous solutions, molybdenum oxyanions exist in the form of monomeric $[MoO_4]^{2-}$ ion, while at pH < 6 and higher molybdenum concentrations, the anion species become protonated and coexists in hepta- or octa- ion forms. At pH 2–6, heptamolybdate anion $Mo_7O_{24}^{6-}$ predominates. This polyanion can be protonated at low pH values forming polynuclear hydrolyzed species such as $Mo_7O_{21}(OH)_3^{3-}$, $Mo_7O_{22}(OH)_2^{4-}$ and $Mo_7O_{23}(OH)^{5-}$ (Atia et al., 2008; Navarro et al., 2003).

It is important to note that the metal species distribution vs. pH may influence metal uptake in such a way that the optimum pH then depends on the total concentration (Navarro et al., 2003).

The sorption mechanism is dependent on the speciation of metal ions as well as on the degree of the protonation of these amine groups. At pH values close to neutral, sorbents with amino groups sorb metal cations by chelation mechanism, while in acidic solutions metal anions can be sorbed through electrostatic interactions with the protonated amine groups (Guibal et al., 1998).

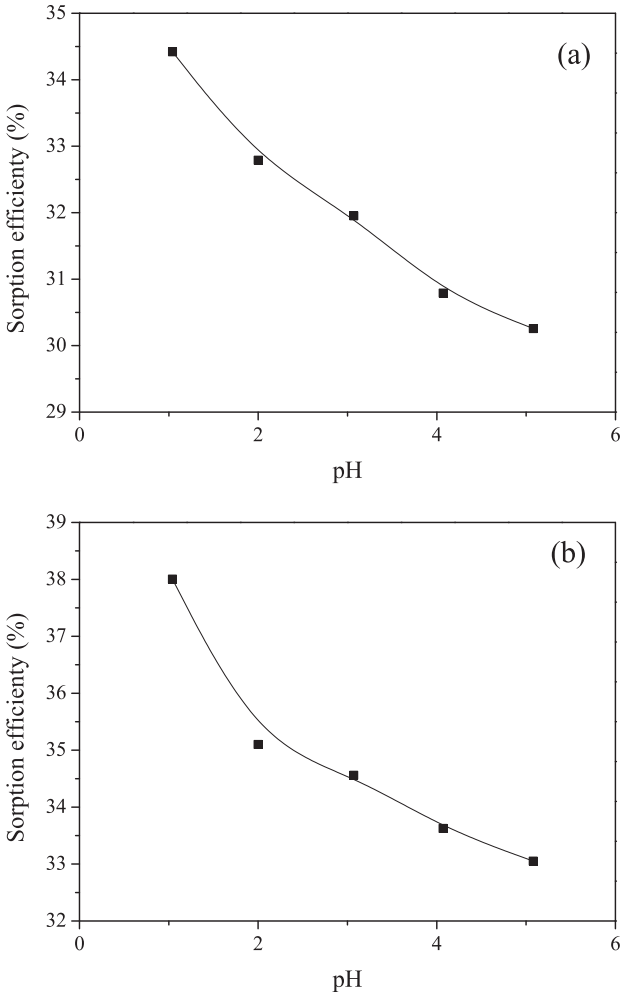

Figure 1 Effect of pH on the Mo(VI) sorption onto PGME-deta at (a) t = 180 min and (b) t = 300 min (C_i = 0.1 M, T = 298 K).

The effect of pH on the Mo(VI) sorption by PGME-deta was investigated at 298 K by varying the pH values of the solution from 1.0 to 5.0 (C_i = 0.1 M) and the results are presented in Fig. 1.

It was observed that the sorption capacity was inversely correlated with the increasing pH value. The similar was already observed for the pertechnetate anions sorption by PGME-deta (Webb and Orr, 1997). Namely, the p*K*a value of amine groups characteristically lies within the range 8–11 (Baker et al., 2010), meaning that the amine groups are fully protonated at pH < 5. Consequently, the degree of protonation slowly decreases with the increase in pH, and the sharp decline of removal efficiency would be expected. It is probable that predominantly hydrogen bonds are being formed between molybdenum oxyanion species and neutral amino groups at pH values higher than 8.

Shen et al. investigated the adsorption mechanism of Cu(II) and Cr(VI) co-existing water system by a series of NH_2-functionalized nano-magnetic polymer adsorbents (NH_2-NMPs) coupled with different multi-amino groups, i.e., ethylenediamine (EDA), diethylenetriamine (DETA), triethylenetetramine (TETA) and tetraethylenepentamine (TEPA) (Shen et al., 2012). However, instead of decreasing the adsorption capacity with the pH increase (expected due to the decrease of protonated amino groups) they observed that there was a flat (plateau) for each curve adsorption capacity-pH value, meaning that besides the electrostatic attraction and ion exchange interactions, coordination interactions might occur in the adsorption process.

As seen from Fig. 1, sorption efficiency declines approximately 5%, i.e., from 34% to ~30% (Fig. 1a) and 38% to ~33% (Fig. 1b.) with pH increase from 1 to 5. Similar to findings of Shen et al., the absence of significant decline of Mo(VI) sorption capacity by PGME-deta with increasing pH (Fig. 1a and b) also might be the consequence of simultaneous occurrence of the electrostatic attraction, ion exchange and coordination.

Navarro and coauthors demonstrated the higher affinity of chitosan for polynuclear species characterized by a high density of anionic charges, attaining maximum sorption capacities for Mo of 7–8 mmol metal g^{-1}. The N content for the investigated chitosan was 6 mmol N g^{-1}, and the total free amine content was 5.2 mmol $-NH_2$ g^{-1} (Navarro et al., 2003). Accordingly, the molar ratio Mo(VI)/amine groups exceeded 1.

The maximum sorption capacity of PGME-deta for Mo (VI) oxyanions in this study was attained at pH 1.0. Considering that such extreme pH values present additional ecological problem that should be avoided, the remaining experiments in this paper were carried out at the pH value of 2.0.

3.3. Effect of contact time

The sorption of Mo(VI) by PGME-deta at pH = 2.0 is shown in Fig. 2, allowing the 24 h contact time for the experiments at room temperature (298 K), investigated in the range of initial Mo(VI) concentrations of 0.01–0.1 M.

The rate of Mo(VI) sorption onto PGME-deta was high within the initial 30 min and the process then gradually slowed down. The plots of Mo(VI) sorption by macroporous PGME-deta were single continuous curves not reaching saturation, except for the lowest initial Mo(VI) concentration (C_i = 0.01 M), indicating the possible multilayer coverage

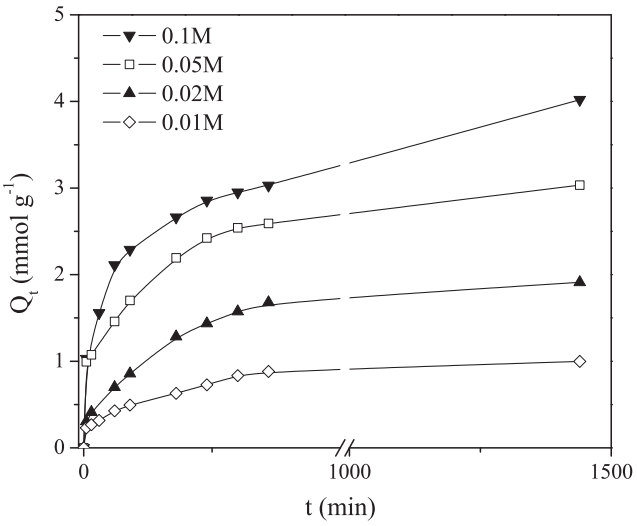

Figure 2 Effect of contact time on the sorption of Mo(VI) on PGME-deta at different initial concentrations (pH = 2.0, T = 298 K).

of Mo(VI) on the copolymer surface (Namasivayam and Sengeetha, 2006). Despite not attaining equilibrium, the Mo (VI) quantity sorbed at C_i = 0.01 M in the absence of mixing at 298 K was 4.02 mmol g^{-1} i.e. the molar ratio Mo(VI)/amine groups was superb 0.80.

3.4. Effect of temperature

The effect of temperature on Mo(VI) ions sorption onto PGME-deta was investigated in the temperature range 298–343 K. The results are shown in Fig. 3. It was observable from the graphs that the sorption of Mo(VI) anions on PGME-deta is dependent on the temperature and the temperature rise promotes Mo(VI) removal.

As the temperature increases from 298 K to 343 K, the maximum experimental sorption capacity of molybdate anions varied from 3.03 to 3.58 mmol g^{-1} after a 6 h period. Also, for

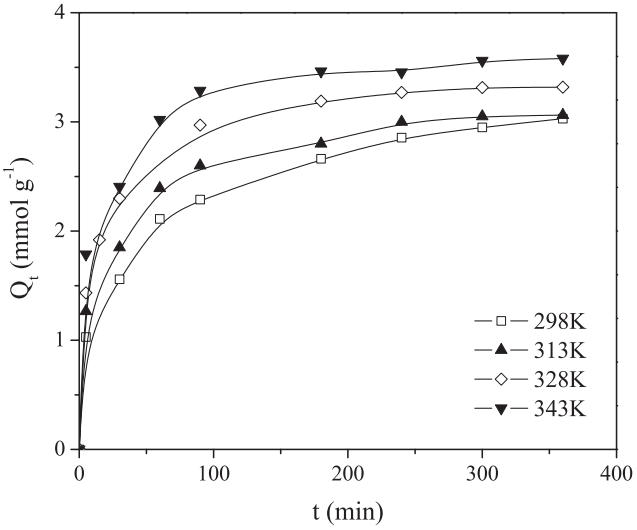

Figure 3 Effect of temperature on Mo(VI) sorption rate on PGME-deta, C_i = 0.1 M.

higher temperatures the maximum sorption capacity was achieved faster, due to an increase in diffusion and ligand chain mobility.

When one takes into account the benefit of the principally enhanced maximum capacity, with temperature, when dealing with the sorption/recovery systems such as in this instance, it is also necessary to consider the added energy cost for heating especially larger bodies of polluted water. A cost vs. benefit study would be required; however, this issue is outside the scope of this paper. The main focus of this study thus remained on the sorption at room temperature.

It was previously published by our group that PGME-deta with 20% crosslinker with the slightly differing relevant characteristics (surface area 29 $m^2\,g^{-1}$, specific pore volume 0.89 $cm^3\,g^{-1}$, pore diameter 212 nm, particle size 150–300 μm, amino groups concentration 6.51 mmol g^{-1}) (Ekmeščić et al., 2012), obtained in the same manner as the PGME-deta with 40% crosslinker, successfully sorbed Mo (VI) oxyanions. The experiments were likewise performed at pH = 2.0, C_i = 0.1 M. The interactions in this system were interpreted based on the overall positive surface charge of PGME-deta and the negative charges of the molybdenum anionic species. It has been established that the amino groups (—NH_2) of PGME-deta are in their protonated cationic form (—NH_3^+) to a high extent in acidic solution, that the copolymer surface is positively charged and that the electrostatic interaction occurs between the sorbent and molybdenum oxyanions as the initial step in the binding mechanism. This resulted in excellent Mo(VI) uptake; the temperature rise was shown to elevate Mo(VI) sorption by the said copolymer with the maximum experimental sorption capacity of 6.10 mmol g^{-1} at 343 K, the molar ratio Mo(VI)/amine groups being 0.94.

3.5. Sorption kinetics

Determination of sorption mechanism and the potential rate-controlling steps are the critical factors for selecting optimum operating conditions of the sorption system. Customarily, sorption is regarded as a quasi-instantaneous mechanism and external mass-transfer resistance as well as intraparticle mass-transfer resistance is prone to be rate-controlling (Guibal et al., 1998). Particularly in the case of the sorption of large molecules, with long contact times to equilibrium, it is believed that the sorption rate is diffusion controlled by boundary layer resistance and/or pore diffusion mass transport (Choy et al., 2004).

Surface-reaction (PFO, PSO, Elovich) and particle diffusion-based (IPD, Bangham, Boyd and McKay's) kinetic models were used to investigate the controlling mechanism of Mo(VI) sorption by PGME-deta. The experimental data obtained for Mo(VI) sorption at various temperatures and initial concentrations were used for calculating the kinetic parameters. Kinetic parameters calculated from surface-reaction and particle diffusion-based models for different initial concentrations and different temperatures are reported in Tables 1 and 2, respectively.

3.5.1. Surface-reaction-based models

The PFO and PSO kinetic models are the most widely used rate equations to describe kinetic parameters of sorption processes from the liquid phase (Ho and McKay, 1998; Ho, 2006).

Table 1 Kinetic parameters for Mo(VI) sorption using PGME-deta at different initial concentrations (pH = 2, T = 298 K, t = 24 h).

C_i (M)	0.1	0.05	0.02	0.01
Q_e (mmol g^{-1})	4.02	3.03	1.91	1.00
Q_e (mg g^{-1})	386	291	183	95.7
PFO				
$k_1 \cdot 10^3$ (min^{-1})	3.38	5.07	5.53	5.30
Q_e^{calc} (mmol g^{-1})	2.82	2.24	1.70	0.84
R^2	0.867	0.959	0.994	0.981
PSO				
$k_2 \cdot 10^3$ (g $mmol^{-1}$ min^{-1})	3.01	5.53	5.90	12.9
h (mmol g^{-1} min^{-1})	0.0522	0.0542	0.0240	0.0141
Q_e^{calc} (mmol g^{-1})	4.16	3.13	2.02	1.04
R^2	0.992	0.997	0.996	0.995
Elovich				
a_e (mmol g^{-1} min^{-1})	0.487	0.502	0.0946	0.0648
b_e (g $mmol^{-1}$)	1.88	2.46	3.08	6.37
R^2	0.977	0.940	0.933	0.928
IPD				
k_{1id} (mmol g^{-1} $min^{-0.5}$)	0.181	0.115	0.0871	0.0399
C_{1id} (mmol g^{-1})	0.618	0.671	0.0738	0.117
R^2	0.987	0.992	0.995	0.994
$k_{1id} \cdot 10^3$ (mg g^{-1} $min^{-0.5}$)	57.6	25.3	14.7	7.16
C_{2id} (mmol g^{-1})	1.89	2.08	1.36	0.737
R^2	0.978	0.982	0.944	0.954
Bangham				
$k_b \cdot 10^3$ (g^{-1})	0.352	0.622	0.271	0.387
α	0.280	0.296	0.568	0.521
R^2	0.990	0.957	0.973	0.950
McKay				
S (min^{-1})	3.45	5.07	5.53	5.30
R^2	0.867	0.959	0.996	0.981

The linearized form of PFO (Eq. (2)) (Ho and McKay, 1998), PSO (Eq. (3)) (Ho, 2006) and Elovich (Eq. (4)) (Önal, 2006) kinetic models used for calculations is as follows:

$$\log\,(Q_e - Q_t) = \log Q_e - \frac{k_1 t}{\ln 10} \tag{2}$$

$$\frac{t}{Q_t} = \frac{1}{k_2 Q_e^2} + \frac{1}{Q_e} t \tag{3}$$

$$Q_t = \frac{\ln a_e b_e}{b_e} + \frac{1}{b_e} \ln t \tag{4}$$

where Q_e is the amount of sorbed Mo(VI) at equilibrium; k_1 is the PFO rate constant; k_2 is the PSO rate constant; h is initial sorption rate from PSO model, calculated as $h = k_2\,Q_e^2$, a_e is the initial sorption rate and b_e is related to the extent of surface coverage and activation energy for chemisorption.

The plots for the PFO and PSO models are shown in Figs. 4 and 5, for different initial concentrations and different temperatures, respectively. The values for Q_e, k_1, k_2 and h were calculated from the plots of $\log(Q_e–Q_t)$ or t/Q_t versus t for each initial metal concentration and temperature and given in Tables 1 and 2.

As can be seen, the rate of removal of Mo(VI) on PGME-deta does not follow the PFO model since the determination

Table 2 Kinetic parameters for Mo(VI) sorption using PGME-deta at different temperatures (pH = 2, C_i = 0.1 M, t = 360 min).

T (K)	298	313	328	343
Q_e (mmol g^{-1})	3.03	3.06	3.32	3.58
Q_e (mg g^{-1})	291	294	318	343
PFO				
$k_1 \cdot 10^3$ (min^{-1})	10.8	15.9	19.1	14.5
Q_e^{calc} (mmol g^{-1})	2.22	2.26	2.34	1.90
R^2	0.981	0.959	0.956	0.926
PSO				
$k_2 \cdot 10^3$ (g mmol^{-1} min^{-1})	15.7	17.2	24.9	25.3
h (mmol g^{-1} min^{-1})	0.014	0.177	0.292	0.333
Q_e^{calc} (mmol g^{-1})	3.12	3.20	3.43	3.66
R^2	0.995	0.998	0.999	0.999
Elovich				
a_e (mmol g^{-1} min^{-1})	0.607	2.21	2.28	5.27
b_e (g mmol^{-1})	2.03	2.36	2.19	2.27
R^2	0.980	0.915	0.990	0.960
IPD				
k_{1id} (mmol g^{-1} min$^{-0.5}$)	0.181	0.190	0.206	0.213
C_{1id} (mmol g^{-1})	0.618	0.842	1.07	1.30
R^2	0.987	0.991	0.980	0.993
$k_{2id} \cdot 10^3$ (mg g^{-1} min$^{-0.5}$)	0.0795	0.0526	0.0379	0.0307
C_{2id} (mmol g^{-1})	1.57	2.12	2.65	3.01
R^2	0.979	0.946	0.926	0.938
Bangham				
$k_b \cdot 10^3$ (g^{-1})	0.339	0.472	0.574	0.742
α	0.290	0.240	0.226	0.196
R^2	0.990	0.977	0.972	0.953
McKay				
S (min^{-1})	10.8	15.9	19.1	14.3
R^2	0.981	0.959	0.956	0.925

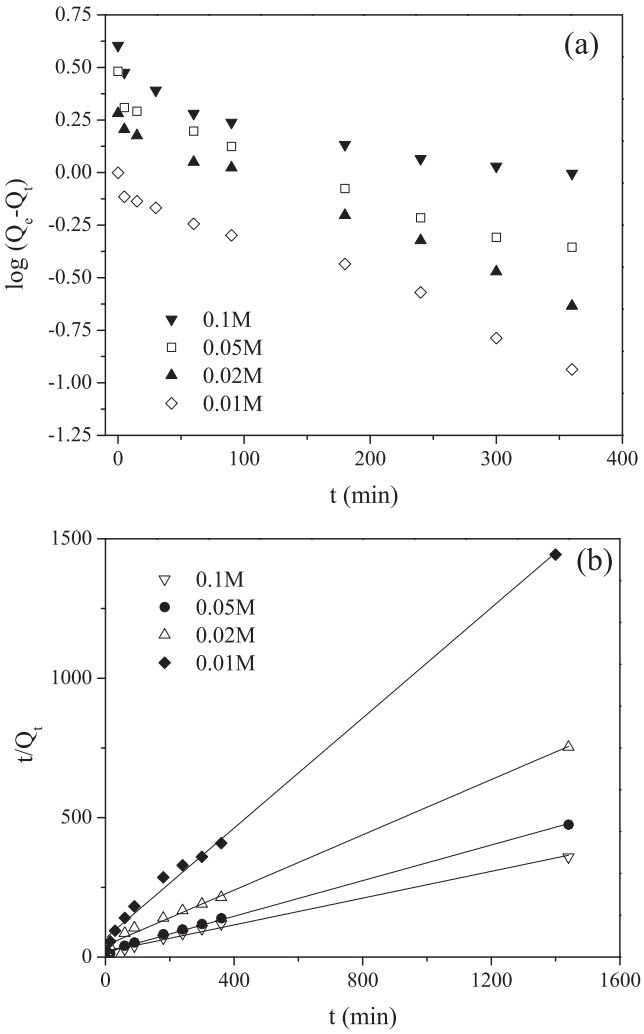

Figure 4 (a) PFO and (b) PSO kinetics for Mo(VI) sorption on PGME-deta (pH = 2, T = 298 K) for indicated initial concentrations.

coefficient values (R^2) were rather low. On the other hand, the calculated Q_e values obtained from PSO model for all investigated concentrations and temperatures agree very well with experimental Q_e ones with $R^2 > 0.99$. Also, from Table 2, it was noted that the initial sorption rate, h, increases with increasing temperature. From this it can be inferred that the kinetics of Mo(VI) anion sorption onto PGME-deta is accurately described by PSO at all time intervals, implying that chemisorption mechanism may play an important role for the sorption of this anion onto PGME-deta, i.e. that sorption rate is controlled by both the sorbent capacity and the sorbate concentration.

The intercept ln a_e b_e/b_e from the Elovich linear equation is regarded as the amount sorbed during the initial fast phase reaction and $1/b_e$ is the sorption rate as a function of time during the slow phase of the reaction (Cáceres et al., 2010).

The low intercept confirms that the equilibrium is reached after extended period of time for sorption of Mo(VI) on PGME-deta. The parameter a_e monotonously decreased with decreasing concentration and monotonously increased with temperature. The b_e values monotonously decreased with the increased initial Mo(VI) concentration, an indication of the lower number of sites available for sorption while the increase in temperature only did not have a significant effect on it (Martins et al., 2014). The magnitude of R^2 was lower for Elovich than for the PSO model, but still rather high, which supports the assumption that chemisorption is the main adsorption controlling mechanism.

3.5.2. Particle diffusion-based models

Most sorption processes take place through multistep mechanism, especially when microporous/mesoporous/macroporous sorbents are used. In the case of a porous adsorbent, the external mass transfer and intraparticle diffusion must be taken into account as well (Ip et al., 2010; Weber and Morris, 1963). In order to determine whether the process rate in the studied sorption system is directed by film and/or pore diffusion, four models were applied: intraparticle (IPD) (Eq. (5), (Wu et al., 2009)), Bangham (Eq. (6), Tütem et al. (1998)), Boyd (Eqs. (7) and (8), Reichenberg (1953)) and McKay's (Eq. (9), Mittal et al. (2005)). The corresponding equations are as follows:

$$Q_t = k_{id} t^{1/2} + C_{id} \tag{5}$$

$$\log \log \left[\frac{C_i}{C_i - C_s Q_t}\right] = \log \left[\frac{k_b C_s}{2.303\ \mathrm{V}}\right] + \alpha \log t \tag{6}$$

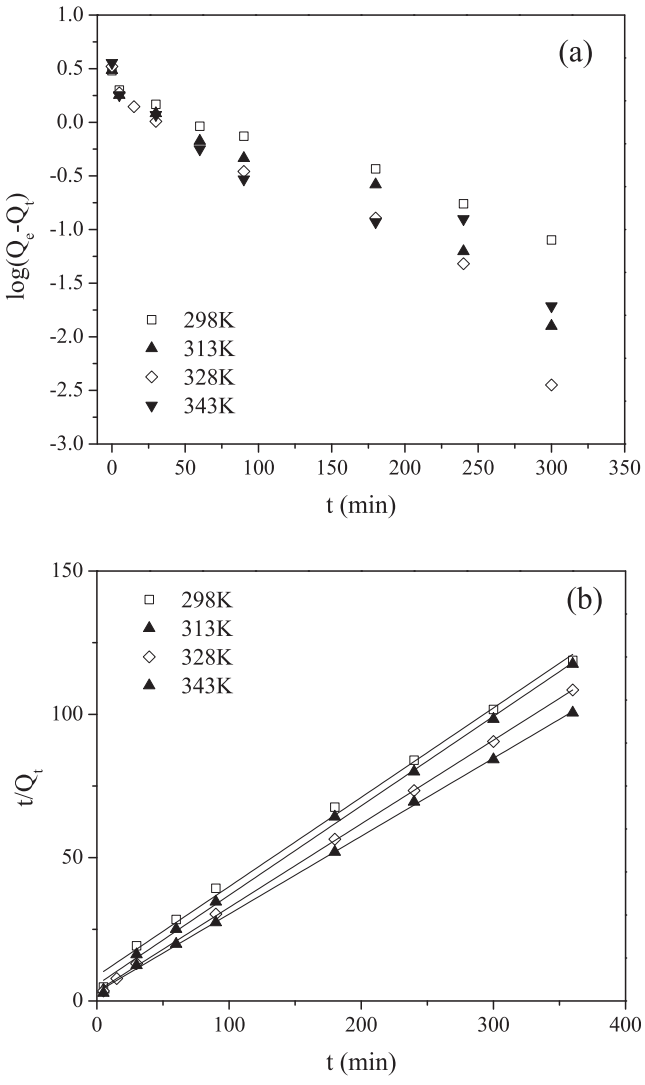

Figure 5 (a) PFO and (b) PSO kinetics for Mo(VI) sorption on PGME-deta (pH = 2, C_i = 0.1 M) for indicated temperatures.

$$Bt = \left(\pi^{\frac{1}{2}} - \left(\pi - \frac{\pi^2 F}{3}\right)^{\frac{1}{2}}\right), \quad F < 0.85 \tag{7}$$

$$Bt = -0.4997 - \ln(1 - F), \quad F > 0.85 \tag{8}$$

$$\log(1 - F) = -\left(\frac{S}{2.303}\right)t \tag{9}$$

where k_{id} is the intraparticle diffusion coefficient; C_{id} is a constant, related to the thickness of the boundary layer; C_s is the sorbent dosage; k_b constant calculated from intercept of linear Bangham's plots; α constant calculated from slope of linear Bangham's plots; Bt is a mathematical function of F; F is the fractional attainment of equilibrium at time t, calculated as $F = Q_t/Q_{e;}$ and S is the rate parameter.

Fig. 6 shows the IPD plots for the Mo(VI) sorption at different initial concentrations and temperatures. The $Q_t - t^{1/2}$ plots are the straight lines and pass near the origin, with high values of R^2. It is observed from Table 2 that intercept of IPD plot increases as the temperature of solution increases from 298 to 343 K. As the value of intercept increases, the effect of the boundary layer thickness also increases (Wu et al., 2009). IPD plots showed two different slopes of the linear plots in two subsequent time intervals, and indicating that two diffusion steps are involved in the Mo(VI) sorption process on PGME-deta (Ofomaja, 2011).

According to IPD model, if the $Q_t - t^{1/2}$ (IPD) plot is a straight line passing through the origin, IPD is the only rate-controlling step in the sorption process (Wu et al., 2009).

There are opinions in the literature that multi-linear $Q_t - t^{1/2}$ plots observed for sorbents with extensive pore size distribution may be the result of the distinctive phases in IPD. It is generally considered that multi-linear plots represent the stages of IPD into the macro-, meso-, and microporous structure of the sorbent (Ip et al, 2010; Porkodi and Kumar, 2007). In our case, the first stage could represent the sorption over the outer surface and in the PGME-deta macropores, rendering it the quickest sorption stage, while the second one could be attributed to the IPD through mesopores. Nonexistence of the third stage could be ascribed to the absence of

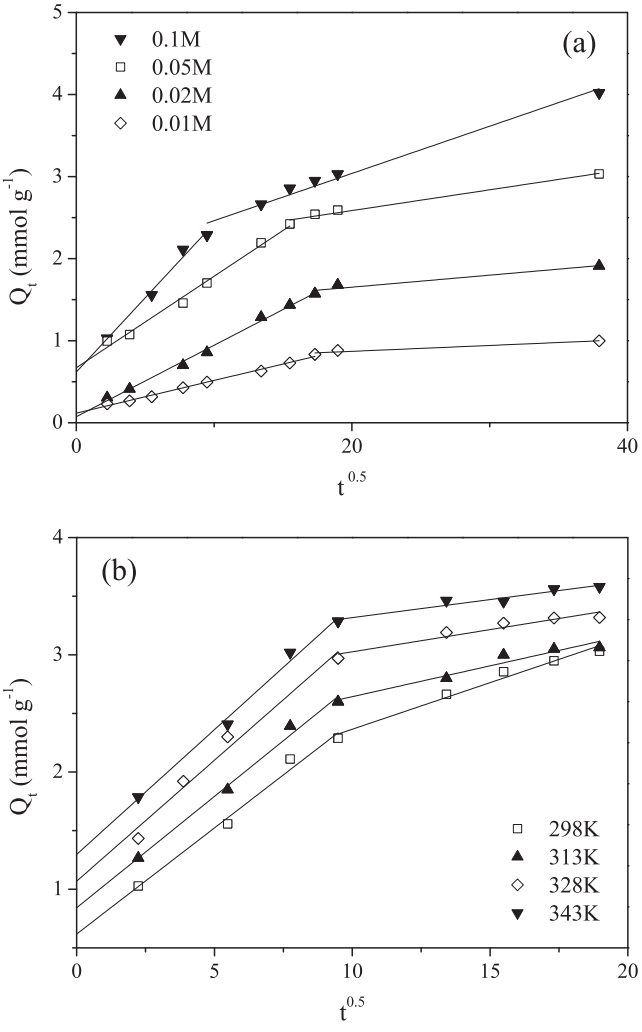

Figure 6 Plots of IPD model for Mo(VI) sorption on PGME-deta at pH = 2 for: (a) different initial concentrations at 298 K, t = 24 h and (b) different temperatures for C_i = 0.1 M, t = 360 min.

micropores in PGME-deta. Additionally, Mo(VI) polynuclear anions species which have remarkably large hydrated radii govern the steric hindrance and access to internal sites (Ip et al., 2010). Over time, the pores for diffusion become smaller, because the Mo(VI) oxyanions diffuse into the inner structure of the sorbents, causing the decrease of the free path of the molecules in the pore as well as pore blockage (Rorrer et al., 1993). Overall, the sufficient macro- and mesopores of PGME-deta provided the effective diffusion channels for Mo (VI) to sorption sites and enhanced the sorption kinetics.

The double logarithmic Bangham's plots were linear with good R^2 values ($R > 0.9$). It was noted that, on increasing the temperature, the value of α decreased and the value of k_b increased. This result confirms that investigated sorption process is pore diffusion controlled.

The kinetic data have been analyzed using the model given by Boyd in order to identify whether external transport or intraparticle transport controls the rate of Mo(VI) sorption on PGME-deta.

The Boyd's plot Bt–t should be linear and pass through the origin when the particle-diffusion is a rate-controlling step of sorption processes; if not, they are governed by film diffusion (Vadivelan and Kumar, 2005). From Fig. 7, it was observed that plots were close to linear and passed quite near the origin, indicating that the sorption rate of Mo(VI) on PGME-deta is governed mainly by IPD mechanism.

Fig. 8 shows typical Mckay's plots at different Mo(VI) concentration and at different temperatures. The $\log(1-F)$ versus t plots were linear in the whole range of the time and passed near the origin. The S values calculated from their slopes and the intercepts are presented in Tables 1 and 2. Thus, it can be deduced that the intraparticle diffusion was a major rate determining mechanism of sorption of Mo(VI) on PGME-deta, with minor influence of film diffusion. Both the initial concentration increase and the temperature elevation enhanced this sorption process.

FTIR-ATR spectra of PGME-deta and the sample with Mo(VI) sorbed (PGME-deta/Mo) were recorded in the frequency range of 4000–400 cm^{-1} and are presented in Fig. 9.

The bands for ester vibrations at ~1720 cm^{-1} [ν(C═O)], the bands characteristic for the crosslinked copolymer at ~1160 cm^{-1} [ν(C—O)], ~1450 cm^{-1} [$\delta(CH_2)$] and ~2950 cm^{-1} [ν(C—H)] are present in both samples.

The wide band at ~3060–3700 cm^{-1} [ν(N—H) + ν(O—H)], the bands at ~1260 cm^{-1} [ν(C—N)], ~1560 cm^{-1} and 1650 cm^{-1} [δ(NH), $\delta(NH_2)$], as well as the band at ~1390 cm^{-1} [ν(NH)] indicate the presence of —NH and —NH_2 groups in PGME-deta as a result of functionalization with diethylenetriamine.

As the consequence of incomplete conversion, the low intensity peaks ascribed to the epoxide ring vibrations at 753 and 806 cm^{-1} for PGME-deta and 752 cm^{-1} for PGME-deta/Mo were detected. In PGME-deta/Mo spectrum the bands at ~1560 cm^{-1}, 1650 cm^{-1} [δ(NH), $\delta(NH_2)$] disappeared, indicating the Mo(VI) binding to PGME-deta. However, the most significant part of the spectra regarding Mo (VI) oxyanions sorption is located in the 1000–700 cm^{-1} region (Mo—O absorption bands) (Guibal et al., 1999). Thus, the clear evidence of the Mo(VI) binding to PGME-deta is the appearance of the vibrations at 660, 713, 902 and 941 cm^{-1} associated with the stretching mode of oxygen linked with

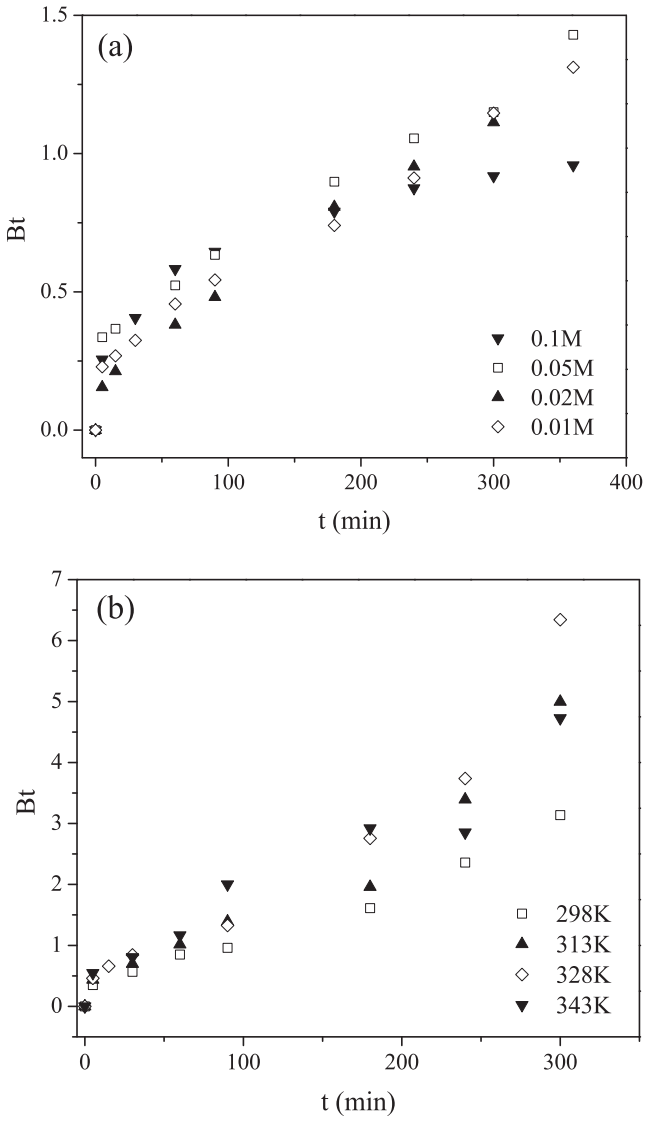

Figure 7 Boyd plots for Mo(VI) sorption by PGME-deta at pH = 2 for: (a) different initial concentrations at 298 K, t = 24 h and (b) different temperatures, C_i = 0.1 M, t = 360 min.

three metal ions, as well as stretching modes of Mo—O—Mo and M═O (Guibal et al., 1999; Phuruangram et al., 2014).

Thus, the absence of characteristic bands for —NH and —NH_2 groups and the presence of the bands in the region of Mo-O absorption in the PGME-deta/Mo spectra indicate that, besides electrostatic interaction, adsorption proceeds partially via coordination.

For further understanding of Mo(VI) sorption by PGME-deta, SEM-EDS (energy-dispersive X-ray spectroscopy) was performed on both surface and cross-section of PGME-deta/Mo(VI) particles. The SEM-EDS analysis confirmed the presence of all expected elements (C, O, N and Mo). The obtained results are presented in Table 3. As can be seen, the N percentage was almost the same on the particles surface and in the cross-section indicating that the reaction of epoxy groups with diethylenetriamine occurs equally on the surface and in the interior of the beads. Furthermore, EDS analysis showed that a significant amount of molybdenum binds to the amino

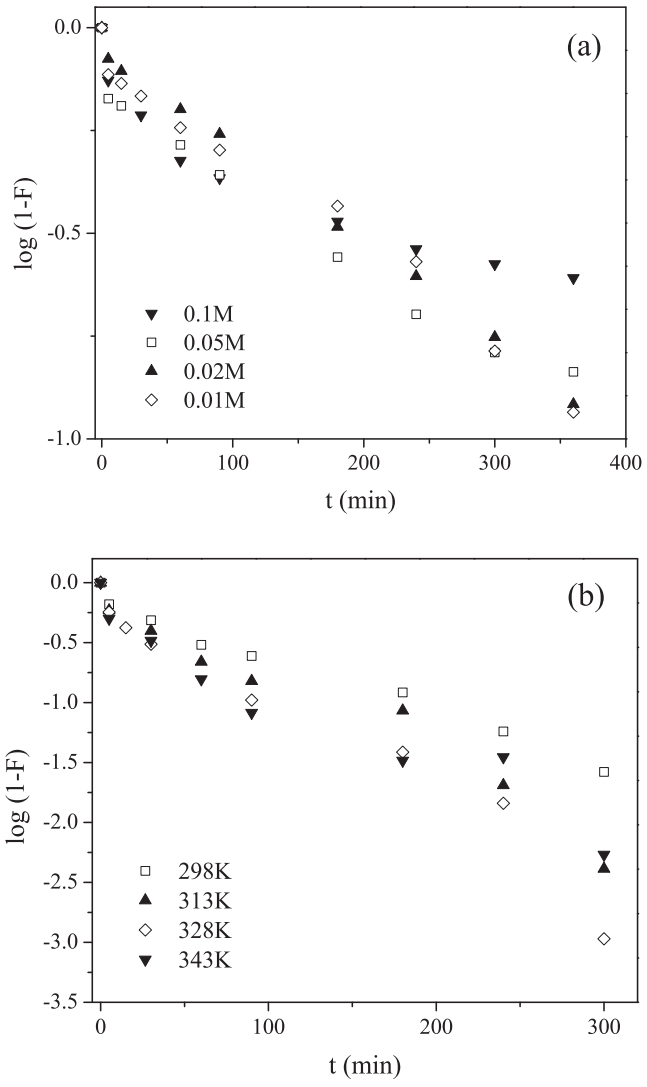

Figure 8 Mckay plots for Mo(VI) sorption by PGME-deta at pH = 2 for: (a) different initial concentrations at 298 K, t = 24 h and (b) different temperatures, C_i = 0.1 M, t = 360 min.

groups on the particle exterior surface (23%) as well as on the interior (20%), thus confirming the significance of the intra-particle diffusion as the controlling step of Mo(VI) sorption by PGME-deta.

3.6. Apparent activation energy of sorption

The activation energy for the PGME-deta/Mo(VI) sorption system can be determined from the linearized Arrhenius equation (Ho and McKay, 1998):

$$\ln k_2 = \ln A - \frac{E_a}{RT} \quad (10)$$

where A is the temperature independent factor (frequency factor) (g mmol^{-1} min^{-1}), E_a is the activation energy (kJ mol^{-1}), T is the temperature (K) and R is the universal gas constant equal to 8.314 J mol^{-1} K^{-1}.

The $\ln k_2$ vs. $1/T$ plot (Fig. 10) was perceived to be linear with satisfactory R^2 value of 0.997 for the concentration of 0.1 M and E_a value for the studied sorption system calculated

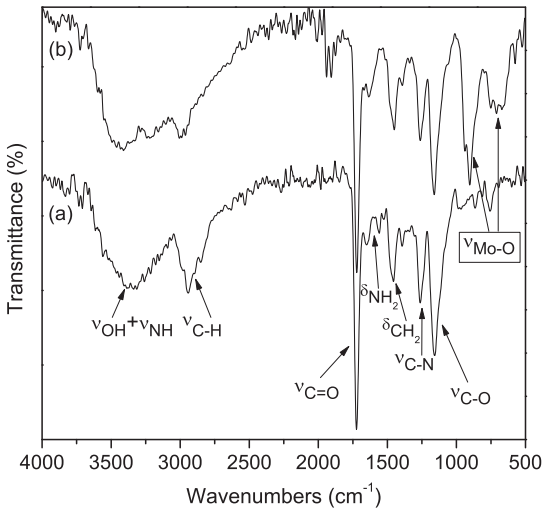

Figure 9 FTIR spectra of the (a) PGME-deta and (b) PGME-deta/Mo(VI).

Table 3 Results of SEM-EDS analysis of PGME-deta/Mo (VI).

Element	Particle surface		Cross-section	
	Weight %	Atomic %	Weight %	Atomic %
C-K	22.65	33.79	23.84	34.38
N-K	9.01	11.52	8.21	10.14
O-K	44.92	50.31	47.91	51.86
Mo-L	23.43	4.38	20.04	3.62

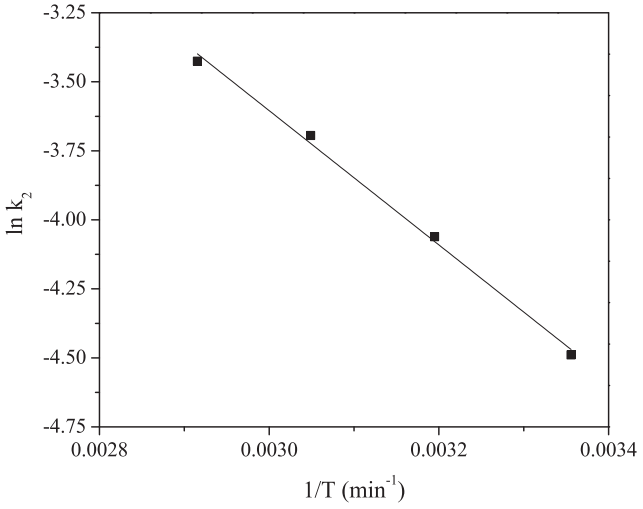

Figure 10 The $\ln k_2$ vs. $1/T$ plot for the PGME-deta/Mo(VI) sorption system.

from the slope was 20.2 kJ mol^{-1}. This parameter's value may offer insights into the sorption mechanism. According to Glasston et al. (1941), when sorption rate is governed by intra-particle diffusion mechanism, activation energy is low and within the range of values of 8–22 kJ mol^{-1}. Bearing in mind that the calculated E_a value was close to the upper limit of the range for diffusion-controlled processes and that the

Table 4 Overview of Mo(VI) uptake with various sorbents.

Sorbent	pH	T (K)	Ci (M)	Q_{max} (mmol/g)	References
Magnetic GMA/DVB/TEP[a]	2	333	$8 \cdot 10^{-3}$	5.6	Atia et al. (2008)
Magnetic GMA/MBA/TEP[b]	2	333	$8 \cdot 10^{-3}$	7.6	Atia et al. (2008)
Maghemite (γ-Fe2O3)	5	306	$1 \cdot 10^{-3}$	0.3	Afkhami and Norooz-Asl (2009)
Nanoparticles					
DAPSH-APTES@SiO_2[c]	5	298	$6.3 \cdot 10^{-3}$	1.2	Sharma et al. (2012)
Zn–Al sulfate layered double hydroxides (LDHs)	7–8	318	$16 \cdot 10^{-3}$	0.53	Ardau et al. (2012)
NaOCl oxidized multiwalled carbon nanotube	7	293	$10 \cdot 10^{-3}$	0.2	Chen and Lu (2014)
Akaganeite (β-FeOOH)	7	333	$0.2 \cdot 10^{-3}$	4.2	Lazaridis et al. (2003)

[a] GMA/DVB/TEP: copolymer of GMA and divinylbenzene (DVB) functionalized with tetraethylenepentamine (TEP).
[b] GMA/MBA/TEP: copolymer of GMA and *N*,*N*-methylenebisacrylamide (MBA) functionalized with tetraethylenepentamine (TEP).
[c] DAPSH-APTES@SiO_2: silica modified 2,6-diacetylpyridine-monosaliciloylhydrazone.

sorption capacity increased with temperature, this may indicate that chemisorption process was rate-controlling as well as pore diffusion.

Thermodynamic considerations of the sorption process of Mo(VI) by PGME-deta previously published (Ekmeščić et al., 2012) confirmed the positive ΔH value and the increase of Mo(VI) sorption with temperature, both the characteristics of chemical adsorption (endothermic process). This was indicative that both mentioned processes took place with chemisorption being predominant, probably due to the transition metal nature of molybdenum. In the course of the sorption process *d* orbitals become filled with free electron pairs from amino or hydroxy groups of PGME-deta.

3.7. Comparison with other sorbents

The literature data on Mo(VI) oxyanions removal include a variety of sorbents, such as activated carbon (Cruywagen and de Wet, 1988; Pagnanelli et al., 2011), soils components (Sabine and Forster, 1998), and pyrite and goethite (Xu et al., 2006). However, diverse experimental conditions make direct comparison of the literature data difficult to achieve. Nevertheless, some of the results are listed in Table 4 as an illustration.

The maximum Mo(VI) sorption capacities of various sorbents reported in the literature cited here lie between approximately 0.2 mmol g^{-1} for NaOCl oxidized multiwalled carbon nanotube (Chen and Lu, 2014) and 7.6 mmol g^{-1} reported for GMA/MBA/TEP, i.e. copolymer of GMA and *N*,*N*-methylenebisacrylamide (MBA) functionalized with tetraethylenepentamine (TEP) (Atia et al., 2008).

The maximum sorption capacity obtained for PGME-deta in this study was 3.58 $mmolg^{-1}$ at 343 K (Table 4), while Atia et al. reported higher maximum sorption capacity of 5.60 mmol/g for similar magnetic copolymer crosslinked with divinyl benzene, i.e. GMA/DVB/TEP (Atia et al., 2008). For the materials listed in Table 4, the kinetic data were best represented by the pseudo-second-order model.

4. Conclusion

As indicated in the relevant studies published to this day, metal speciation is exceptionally important in the case of ion-exchange processes entailed in the recovery of anionic metal forms by protonated amine groups.

Macroporous crosslinked GMA based copolymer functionalized via ring-opening reaction of the pendant epoxy groups with diethylenetriamine (PGME-deta) was tested as a sorbent for the removal of polynuclear Mo(VI) oxyanions from aqueous solutions in batch static experiments with the respect to pH, temperature, contact time and initial concentration. The sorption capacity of Mo(VI) ions was inversely correlated with increasing pH values, with the maximal value at pH 1.0. The increase of the uptake as the pH value decreased may be attributed to electrostatic interaction between the PGME-deta particle with its protonated amino groups and the negative Mo(VI) oxyanions.

Kinetics of Mo(VI) adsorption onto macroporous PGME-deta was investigated for different initial concentrations at room temperature observing a 24 h-period, as well as in the temperature range 298–343 K allowing the contact time to run for 6 h. The temperature rise obviously promoted Mo(VI) removal.

The kinetic data were thoroughly analyzed using seven kinetic models [PFO, PSO, Elovich, IPD, Bangham, Boyd and Mckay] demonstrating that the Mo(VI) sorption by PGME-deta obeyed the PSO kinetic model, which suggests that the sorption rate is controlled by both sorbent capacity and sorbate concentration. Particle diffusion-based models revealed the strong influence of the intraparticle diffusion and porosity of PGME-deta.

Acknowledgments

This work was supported by the Ministry of Education, Science and Technological Development of the Republic of Serbia (Projects III 43009, III 45001 and ON 172018).

References

Afkhami, A., Norooz-Asl, R., 2009. Removal, preconcentration and determination of Mo(VI) from water and wastewater samples using maghemite nanoparticles. Colloid. Surf. A 346 (1–3), 52–57.

Al-Dalama, K., Aravind, B., Stanislaus, A., 2005. Influence of complexing agents on the adsorption of molybdate and nickel ions on alumina. Appl. Catal. 296 (1), 49–53.

Ardau, C., Frau, F., Dore, E., Lattanzi, P., 2012. Molybdate sorption by Zn–Al sulphate layered double hydroxides. Appl. Clay Sci. 65–66, 128–133.

Atia, A.A., Donia, A.M., Awed, H.A., 2008. Synthesis of magnetic chelating resins functionalized with tetraethylenepentamine for adsorption of molybdate anions from aqueous solutions. J. Hazard. Mater. 155 (1–2), 100–108.

Baker, M.G., Lalonde, S.V., Konhauser, K.O., Foght, J.M., 2010. Role of extracellular polymeric substances in the surface chemical reactivity of Hymenobacter aerophilus, a psychrotolerant bacterium. Appl. Environ. Microbiol. 76 (1), 102–109.

Cáceres, L., Escudey, M., Fuentes, E., Baez, M.E., 2010. Modeling the sorption kinetic of metsulfuron-methyl on Andisols and Ultisols volcanic ash-derived soils: kinetics parameters and solute transport mechanisms. J. Hazard. Mater. 179 (1–3), 795–803.

Chen, Y.C., Lu, C., 2014. Kinetics, thermodynamics and regeneration of molybdenum adsorption in aqueous solutions with NaOCl-oxidized multiwalled carbon nanotubes. J. Ind. Eng. Chem. 20 (4), 2521–2527.

Choy, K.K.H., Porter, J.F., McKay, G., 2004. Intraparticle diffusion in single and multicomponent acid dye adsorption from wastewater onto carbon. Chem. Eng. J. 103 (1–3), 133–145.

Cruywagen, J.J., de Wet, H.F., 1988. Equilibrium study of the adsorption of molybdenum(VI) on activated carbon. Polyhedron 7 (7), 547–556.

Ekmeščić, B., Maksin, D., Suručić, Lj., Marković, J., Marković, D., Vuković, Z., Onjia, A., Nastasović, A., 2012. Thermodynamics of molybdenum adsorption onto porous copolymer, "Physical Chemistry" 2012–11th International Conference on Fundamental and Applied Aspects of Physical Chemistry, 24th–28th September, Belgrade, Republic of Serbia, 2011.

Glasston, S., Laidler, K.J., Eyring, H., 1941. The Theory of Rate Processes: The Kinetics of Chemical Reactions, Viscosity, Diffusion and Electrochemical Phenomena. McGraw-Hill, New York.

Guibal, E., Milot, C., Tobin, J.M., 1998. Metal-anion sorption by chitosan beads: equilibrium and kinetic studies. Ind. Eng. Chem. Res. 37 (4), 1454–1463.

Guibal, E., Milot, C., Eterradossi, O., Gauffier, C., Domard, A., 1999. Study of molybdate ion sorption on chitosan gel beads by different spectrometric analyses. Int. J. Biol. Macromol. 24 (1), 49–59.

Hercigonja, R.V., Maksin, D.D., Nastasović, A.B., Trifunović, S.S., Glodić, P.B., Onjia, A.E., 2012. Adsorptive removal of technetium-99 using macroporous poly(GMA-*co*-EGDMA) modified with diethylene triamine. J. Appl. Polym. Sci. 123 (2), 1273–1282.

Ho, Y.S., McKay, G., 1998. Sorption of dye from aqueous solution by peat. Chem. Eng. J. 70 (2), 115–124.

Ho, Y.S., 2006. Review of second-order models for adsorption systems. J. Hazard. Mater. 136 (3), 681–689.

Ip, A.W.M., Barford, J.P., McKay, G., 2010. A comparative study on the kinetics and mechanisms of removal of Reactive Black 5 by adsorption onto activated carbons and bone char. Chem. Eng. J. 157 (2–3), 434–442.

Jovanović, S., Nastasović, A., Jovanović, N., Jeremić, K., Savić, Z., 1994. The influence of inert component composition on the porous structure of glycidyl methacrylate/ethylene glycol dimethacrylate copolymers. Angew. Makromol. Chem. 219 (1), 161–168.

Lazaridis, N.K., Jekel, M., Zouboulis, A.I., 2003. Removal of Cr(VI), Mo(VI), and V(V) ions from single metal aqueous solutions by sorption or nanofiltration. Sep. Sci. Technol. 38 (10), 2201–2219.

Maksin, D.D., Nastasović, A.B., Milutinović-Nikolić, A.D., Suručić, Lj.T., Sandić, Z.P., Hercigonja, R.V., Onjia, A.E., 2012. Equilibrium and kinetics study on hexavalent chromium adsorption onto diethylene triamine grafted glycidyl methacrylate based copolymers. J. Hazard. Mater. 209–210, 99–110.

Martins, R.J.E., Vilar, V.J.P., Boaventura, R.A.R., 2014. Kinetic modelling of cadmium and lead removal by aquatic mosses. Braz. J. Chem. Eng. 31 (1), 229–242.

Mittal, A., Krishnan, L., Gupta, V.K., 2005. Removal and recovery of malachite green from wastewater using an agricultural waste material, de-oiled soya. Sep. Purif. Technol. 43 (2), 125–133.

Namasivayam, C., Sengeetha, D., 2006. Removal of molybdate from water by adsorption onto ZnCl2 activated coir pith carbon. Bioresour. Technol. 97 (10), 1194–1200.

Nastasović, A., Jovanović, S., Đorđević, D., Onjia, A., Jakovljević, D., Novaković, T., 2004. Metal sorption on macroporous poly(GMA-*co*-EGDMA) modified with ethylene diamine. React. Funct. Polym. 58 (3), 139–147.

Nastasović, A., Jakovljević, D., Sandić, Z., Đorđević, D., Malović, Lj., Kljajević, S., Marković, J., Onjia, A., 2007. Amino-functionalized glycidyl methacrylate based macroporous copolymers as metal ion sorbents. In: Barroso, M.I. (Ed.), Reactive and Functional Polymers Research Advances. Nova Science Publishers Inc., New York, pp. 79–112.

Navarro, J., Guzmán, J., Saucedo, I., Revilla, J., Guibal, E., 2003. Recovery of metal ions by chitosan: sorption mechanisms and influence of metal speciation. Macromol. Biosci. 3, 552–561.

Ofomaja, A.E., 2011. Kinetics and pseudo-isotherm studies of 4-nitrophenol adsorption onto mansonia wood sawdust. Ind. Crop. Prod. 33 (2), 418–428.

Önal, Y., 2006. Kinetics of adsorption of dyes from aqueous solution using activated carbon prepared from waste apricot. J. Hazard. Mater. 137 (3), 1719–1728.

Pagnanelli, F., Ferella, F., de Michelis, I., Vegliò, F., 2011. Adsorption onto activated carbon for molybdenum recovery from leach liquors of exhausted hydrotreating catalysts. Hydrometallurgy 110 (1–4), 67–72.

Porkodi, K., Kumar, V.K., 2007. Equilibrium, kinetics and mechanism modeling and simulation of basic and acid dyes sorption onto jute fiber carbon: Eosin yellow, malachite green and crystal violet single component systems. J. Hazard. Mater. 143 (1–2), 311–327.

Reichenberg, D., 1953. Properties of ion-exchange resins in relation to their structure. III. Kinetics of exchange. J. Am. Chem. Soc. 75, 589–597.

Phuruangrat, A., Ekthammathat, N., Kuntalue, B., Dumrongrojthanath, P., Thongtem, S., Thongtem, T., 2014. Hydrothermal synthesis, characterization, and optical properties of Ce Doped Bi_2MoO_6 nanoplates. J. Nanomater. http://dx.doi.org/10.1155/2014/934165.

Rorrer, G.L., Hsien, T.Y., Way, J.D., 1993. Synthesis of porous-magnetic chitosan beads for removal of cadmium ions from wastewater. Ind. Eng. Chem. Res. 32 (9), 2170–2178.

Sabine, G., Forster, H.S., 1998. Factors affecting molybdenum adsorption by soils and minerals. Soil Sci. 163 (2), 109–114.

Sharma, K.R., Pandey, A., Gulati, S., Adholeya, A., 2012. Silica modified with 2,6-diacetylpyridine-monosalicyloylhydrazone: a novel and selective organic–inorganic sorbent for separation of molybdenum ions in a newly designed reactor. Chem. Eng. J. 210 (1), 490–499.

Shen, H.H., Pan, S., Zhanga, Y., Huang, X., Gong, H., 2012. A new insight on the adsorption mechanism of amino-functionalized nano-Fe_3O_4 magnetic polymers in Cu(II), Cr(VI) co-existing water system. Chem. Eng. J. 183, 180–191.

Soetan, K.O., Olaiya, C.O., Oyewole, O.E., 2010. The importance of mineral elements for humans, domestic animals and plants: a review. Afr. J. Food Sci. 4 (5), 200–222.

Tütem, E., Apak, R., Ünal, C.F., 1998. Adsorptive removal of chlorophenols from water by bituminous shale. Water Res. 32 (8), 2315–2324.

Vadivelan, V., Kumar, V.K., 2005. Equilibrium, kinetics, mechanism, and process design for the sorption of methylene blue onto rice husk. J. Colloid Interf. Sci. 286 (1), 90–100.

Webb, P.A., Orr, C., 1997. Analytical Methods in Fine Particle Technology. Micromeritics Instrument Corporation, Norcross, Georgia.

Weber, W.J., Morris, J.C., 1963. Kinetics of Adsorption on Carbon from Solution. J. Sanitary Eng. Div. 89 (2), 31–60.

World Health Organization (WHO), 2011. Guidelines for drinking-water quality, Fourth edition. Available on: <http://whqlibdoc.who.int/publications/2011/9789241548151_eng.pdf> (accessed June 18th, 2015).

Wu, F.C., Tseng, R.L., Juang, R.S., 2009. Initial behavior of intraparticle diffusion model used in the description of adsorption kinetics. Chem. Eng. J. 153 (1–3), 1–8.

Xu, N., Christodoulatos, C., Braida, W., 2006. Adsorption of molybdate and tetrathiomolybdate onto pyrite and goethite: effect of pH and competitive anions. Chemosphere 62 (10), 1726–1735.